JOURNAL OF MATERIALS SCIENCE 18 (1983) 1731–1742

Effect of stress triaxiality on neck propagation during the tensile stretching of solid polymers

C. G'SELL, N. A. ALY-HELAL
Laboratoire de Physique du Solide (L.A. CNRS No 155), Ecole des Mines, Parc de Saurupt, 54042, Nancy Cedex, France

J. J. JONAS
Department of Mining and Metallurgical Engineering, McGill University, 3450 University Street, Montreal, H3A-2A7, Canada

Cylindrical samples of high density polyethylene were tested in tension at 21° C and a nominal strain rate of 8.5×10^{-4} sec^{-1}. The occurrence of necking in the centre of the specimens was provoked by the introduction of area defects of various sizes. The stabilization of this constriction and its propagation towards the ends of the specimens was studied photographically. An analytical method for the description of neck development is outlined, based on the use of strain and strain rate gradients. The times corresponding to neck initiation and stabilization are shown to be associated with critical values of the local strain hardening coefficient of the material. The role of area, strength and temperature inhomogeneities in the kinetics of strain localization is discussed. A further inhomogeneity term based on the axial variation of the Bridgman triaxiality factor F_T is introduced. It is shown that the transverse compressive stresses associated with the shoulders of the neck can play a significant role in neck propagation in otherwise homogeneous materials.

1. Introduction

The stretching process is of considerable importance in polymer engineering as it is involved in the sequential biaxial orientation of plastic films for magnetic tapes, as well as in the cold drawing of textile or industrial polymer fibres. The objective of these techniques is to produce a final film or fibre of uniform cross-section in which the tensile strength is considerably higher than that of the original, unoriented polymer. Although necking usually takes place, leading to strain localization, this type of plastic instability does not lead to rupture, unlike the case of metals, as long as the stretching parameters are appropriately controlled. Instead, the neck stabilizes, after which a deformation wave is propagated away from the initial constriction. Each portion of the material reached by this wave is reduced in section by the natural draw ratio, which is considered to be a material characteristic for a given temperature and thermochemical history [1, 2].

The influence of the structural parameters of the polymer on its natural draw ratio has already received some attention [3]. However, the kinetics of neck propagation have not been considered in detail, although analytical treatments have been published dealing with the flow of metals during analogous forming operations [4–6]. It was, therefore, the aim of the present investigation to develop a quantitative description of the initiation, stabilization and propagation of the area reduction in solid polymers. The study consisted of three parts: (i) first, the material coefficients were established under constant true strain rate conditions (this part of the investigation has already been published [7, 8]); (ii) second, careful obser-

0022–2461/83 $03.00 + .12

vations were made of the neck propagation process during the stretching of polymer bars [9, 10]; and finally, (iii) computer simulations of strain localization were performed [9, 10], using the material coefficients previously determined, and these were improved until the experimental observations were accurately reproduced. The details of the experimental and computational techniques will be reported elsewhere [10], and the present paper is concerned instead with a description of some of its more unusual features. One such feature is the approach used to account for the presence of stress triaxiality in the vicinity of cross-sectional gradients, and in particular the manner in which the well-known Bridgman correction [11] is adapted to allow for the presence of tranverse stresses at the shoulders of the neck. Unlike the transverse tensile stresses generated at the root of the neck in the classical treatment, these are compressive in nature.

2. Experimental procedure and results

2.1. Specimen preparation

High density polyethylene (HDPE) was chosen as the model semicrystalline polymer in the present study, in part because it has already been the subject of previous investigations of the necking process [12–16]. The material selected was produced by Union Carbide Limited, Canada, and is available commercially as grade DFDY 6130, natural 77. Its physical and macromolecular characteristics are summarized in Table I. The rather high polydispersity ($\bar{M}_w/\bar{M}_n \simeq 13$) was introduced by the manufacturer with the view of conferring on the product an enhanced fracture toughness, even under fairly low temperature conditions. The material was provided in the form of cylindrical rods, 20 mm in diameter, which had been especially extruded for this study by Plastifab Inc. of Montreal*. This forming process was preferred over injection moulding, for it minimizes the growth of internal stresses, as well as the degree of molecular orientation.

Tensile specimens were machined from these rods on a suitable lathe according to the shape depicted in Fig. 1. The gauge section was cylindrical, with an overall length L_0 and a diameter D_0. In order to provoke neck nucleation at a particular site, a central "geometrical defect" [17] was machined into each specimen of length $L_d = L_0/10$. Various defect amplitudes were investigated, which, henceforth, will be referred to in terms of the relative reduction of gauge length cross-section $(A_0 - A_d)/A_0 = (D_0^2 - D_d^2)/D_0^2$. The most common defect amplitude was 4%, but samples were also prepared with amplitudes varying from 0 to 11% [9]. As discussed in more detail elsewhere [18], the behaviour of such geometric defects is equivalent to that of specimens containing strength defects of equal amplitude.

2.2. *In-situ* observation of stretching

The HDPE specimens were continuously stretched by means of a hydraulic, closed-loop, MTS machine equipped with an environmental chamber maintained at -20, $+21$ or $+60°$ C. Only low elongation rates were employed (nominal strain rates $\dot{\epsilon}_N = (1/L_0)(dL/dt)$ between 10^{-5} and 10^{-2} sec^{-1}), in order to ensure that the observed propagation could not be attributed to adiabatic heating effects [19, 20]. The evolution of the specimen profile during a test was followed photographically with the aid of a NIKKORMAT camera mounted facing the sample and connected by a lead to the chart recorder of the tensile machine. In this way, each photograph was associated with a precise overall elongation, measured in the loaded condition.

In order to produce sufficient data for a quantitative description of the necking process, three types of experiments were performed. In the first, the effect of the amplitude of the geometric

TABLE I Physical characteristics of the material selected

Characteristic	Value	Unit
Specific mass	0.956	g cm^{-3}
Melt index (ASTM D 1238, cond E)	0.15	g (10 min)$^{-1}$
Average molecular weight determined by GPC (solvent: trichlorobenzene, 150° C)		
$\bar{M}_w$	192 200	g mol^{-1}
$\bar{M}_n$	14 500	g mol^{-1}
Estimated weight per cent crystallinity	70%	

*The authors are indebted to Mr Mario di Orio of Plastifab Inc. for providing this service.

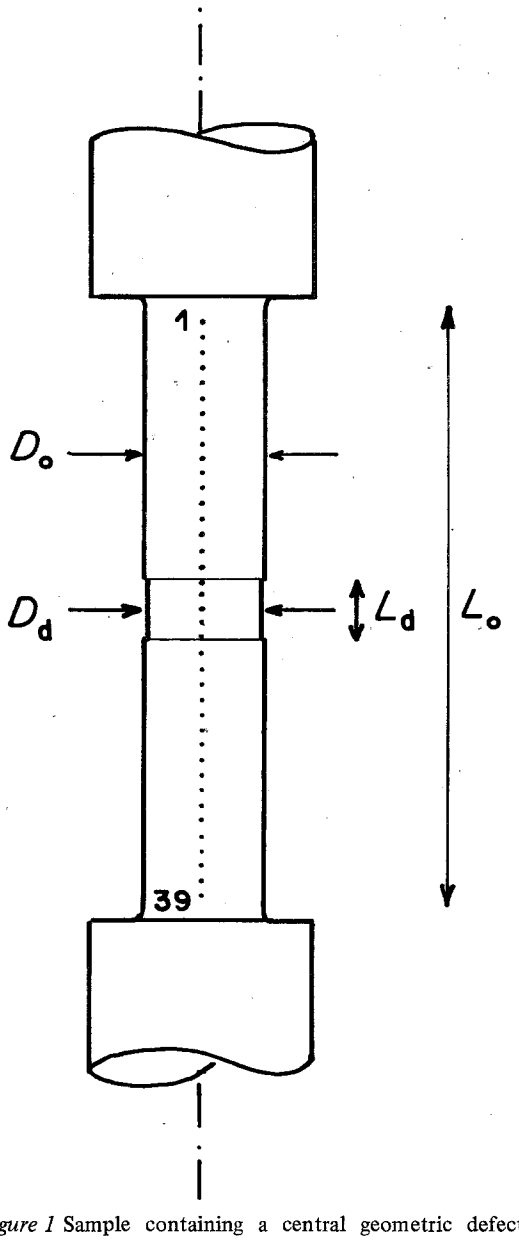

Figure 1 Sample containing a central geometric defect used in the stretching experiments.

defect was investigated; in the second, the strain rate was varied over the experimental range; and in the third, the influence of temperature was determined. In addition, a further series of tests were performed in which a deformation defect was introduced, so that the effect of "hammer blows" [17], and of mechanical damage to the gauge length could be assessed. As stated above, the results of these tests will be described in detail elsewhere [10]. Here we will concern ourselves solely with those aspects of neck propagation which were common to all the tests.

A typical set of specimen profiles, showing the evolution of the neck, is presented in Fig. 2. For the present purpose, the extent of necking is characterized by the maximum true strain, i.e. by the strain associated with the reduction in the sample diameter at the minimum cross-section. Since the specific volume of HDPE stays nearly constant during plastic deformation [15], the true strain is given to a good approximation by $\epsilon \simeq 2 \ln (D_0/D)$, where D_0 and D are the initial (unloaded) and current (loaded) values of the local diameter. This test was carried out at room temperature (21° C), at a crosshead speed of 0.033 mm sec^{-1} ($\dot{\epsilon}_N = 8.5 \times 10^{-4}$ sec^{-1}), on a sample containing a geometric defect of 3.96%. Prior to testing, the surface of each sample was marked with a set of 39 points, which were spaced 1 mm apart along the 40 mm gauge length. These markers permitted the evolution of the strain gradient $\lambda \equiv \partial\epsilon/\partial x|_t$ to be followed at different coordinates x along the specimen during a given tensile experiment.*

It can be seen that the large initial reduction in the minimum cross-section requires about 20 mm of crosshead travel (i.e. an overall elongation of around 50%), after which the constriction is substantially stabilized. Following neck stabilization, the propagation of the constriction takes place during a further 80 mm of crosshead travel (about 200% of overall elongation), although complete propagation to the sample shoulders was not induced, as it would have required still another 180 mm of grip travel (i.e. about 450% of overall elongation), and therefore, a total piston displacement which could not be attained in the current configuration of the machine.

2.3. Evolution of the force and neck strain during stretching

The force against extension curve for this test (Fig. 3a) is characterized by a load maximum at an extension of about 4 mm, which corresponds

*Instability analyses, such as those referred to here [6, 17, 18] are generally expressed in terms of Lagrangian or *specimen* coordinates. That is, in the strain gradient $\partial\epsilon/\partial x|_t$, x refers to a specimen coordinate which is fixed to a specific material element; it does not change during straining, even though the element itself is moving and changing its shape. This is because the true strain ϵ is only known with respect to the *material* cross-section of interest and not with respect to a cross-section fixed in *laboratory* space.

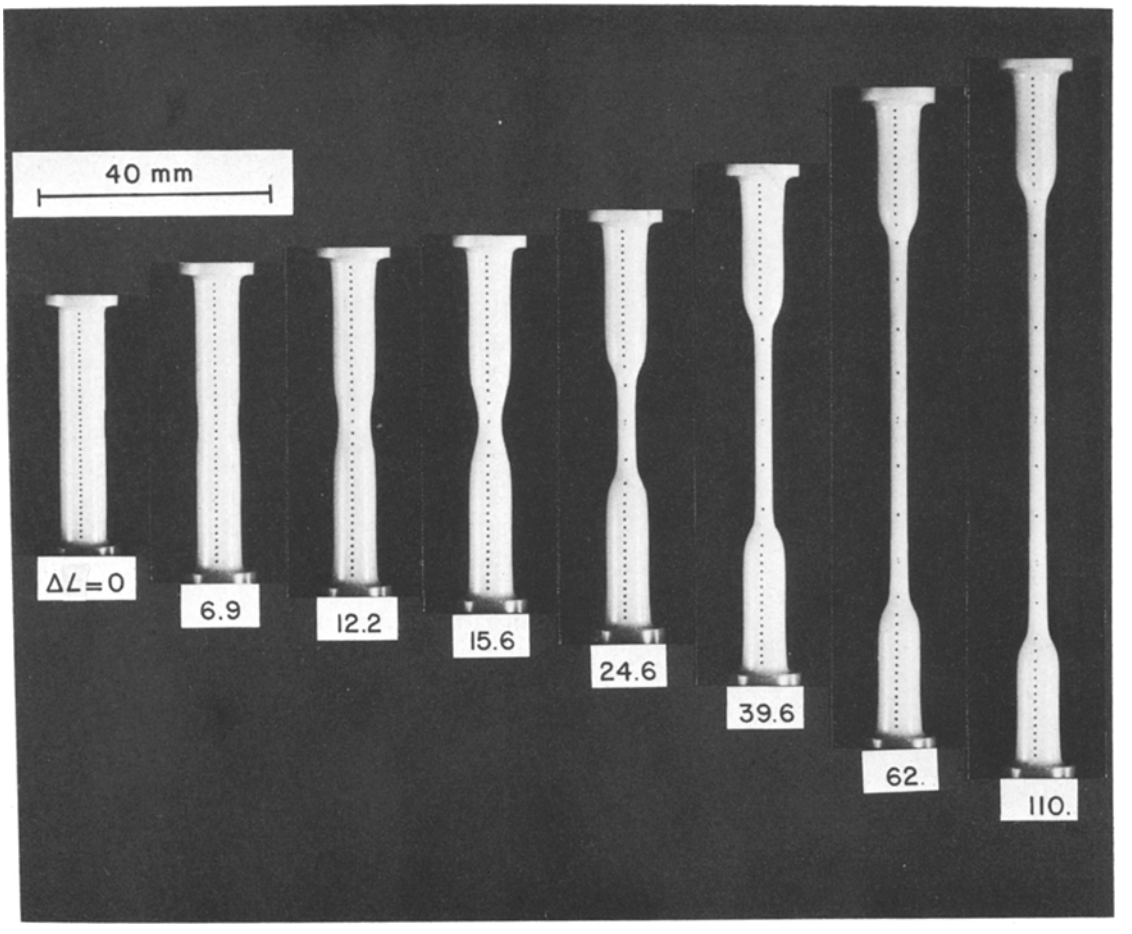

Figure 2 Specimen profiles at increasing elongations in the presence of a geometric defect of 3.96%.

to an overall elongation of 10%, followed by gradual "unloading" to about two-thirds of the maximum force at an extension of 17 mm. (42.5% overall elongation). Thus the period of rapid development of the initial neck corresponds quite closely with the unloading interval; this is because the rate of cross-section decrease at the neck is greater than the rate of local strengthening due to molecular orientation [21]. As will be seen below, this is equivalent to the condition $\gamma_{neck} < 1$, where $\gamma = (\partial \ln \sigma / \partial \epsilon)_{\dot{\epsilon}}$ is the normalized strain hardening rate at constant true strain rate [4]. Following stabilization of the neck, the load increases slowly, while the constriction is gradually propagated towards the ends of the sample. During the propagation period, $\gamma_{neck} \geqslant 1$, while $\gamma < 1$ in the regions through which the constriction is travelling, that is in the current shoulders of the neck. As illustrated elsewhere [10], the depth of the load drop is largely dependent on specimen perfection, whereas the width of the peak (and therefore the length of time required to form the neck) decreases as the magnitude of the defect increases, and vice versa. Thus, the presence of a geometric defect (or of a "strength" defect due to a local temperature increase, for example), aids the process of local orientation, in contrast to the case of metal forming, where appreciable area or strength defects hinder material formability [22].

The evolution of the neck diameter during stretching is illustrated in Fig. 3b, together with the local value of the draw ratio, l/l_0, where l is the current distance between markers situated in the vicinity of the neck, and $l_0 = 1$ mm is the initial separation of the markers. It is evident that, although most of the neck strain is produced during the first 20 mm of crosshead movement (about 50% overall elongation), the neck continues to deform during the propagation interval, so that the limiting draw ratio of about 8 is only attained gradually, and not at the moment of "neck

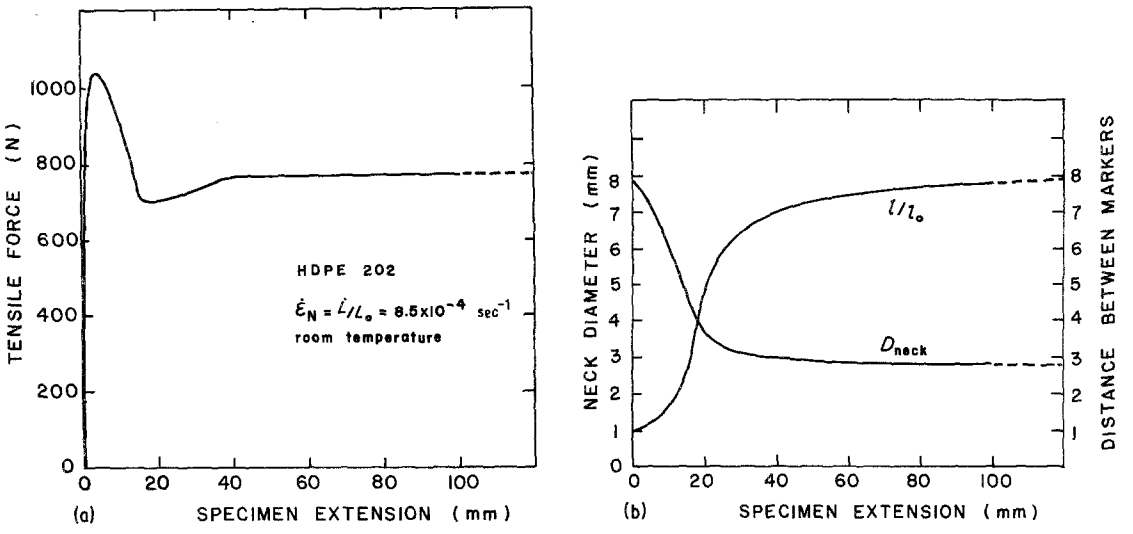

Figure 3 (a) Experimental force-extension curve for the HDPE specimen of Fig. 2. (b) Evolution of the minimum diameter during stretching and of the normalized distance between two consecutive markers l/l_0. The measurements were taken in the central portion of the sample, which contained an area defect of 3.96.

stabilization". Thus, the natural draw ratio is not a real material constant, but can be seen to be an approximate parameter. Moreover, although the rate of increase in draw ratio diminishes to a low value at $\Delta L = 20$ mm, it begins to decrease much earlier, namely, at $\Delta L = 16$ mm, where there is a point of inflection. A similar inflection point is apparent somewhat earlier in the D_{neck} against ΔL curve. These points of inflexion are not attained simultaneously, although they both correspond to the onset of neck stabilization, because the definition of the onset of stabilization depends on whether it is the local diameter or elongation which is chosen for reference [18].

The matter of neck stabilization can also be related to a comparison of the true strains in neighbouring regions of the specimen. Some strain data calculated from the instantaneous diameters at the various markers are illustrated in Fig. 4. Here it can be seen that a neck strain of about 1.8 to 2.0 is first reached at marker 20 at the centre of the defect, and then at markers 19 and 18, which are still within the original geometric defect. The slices situated in the unreduced portion of the sample (i.e. numbers 14 to 17) are successively attained by the deformation wave associated with the propagation of the constriction, but only after much larger specimen extensions. It is of interest that, even at the end of the experiment, slices 1 to 13, i.e. those between the neck and the specimen ends, have not been "drawn" to their limiting size, even though they have cross-sections (and therefore apparent strengths) equal to those of slices 14 to 17. A possible explanation of this anomaly will be advanced below, after a more general consideration of the factors controlling neck growth and stabilization.

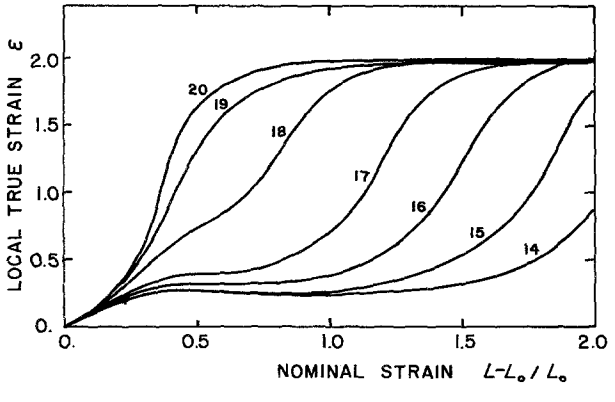

Figure 4 Evolution of the local true strain during stretching at different points along the axis of the tensile bar. The markers were originally 1 mm apart, with number 1 located at the uppermost end of the specimen in Fig. 2, and number 20 located near the centre, within the central region of reduced cross-section.

3. Analytical description of the necking process in solid polymers

3.1. Development of strain gradients

The factors determining the rate of development of strain and strain rate gradients during the deformation of metals are now fairly well understood [6, 17, 18, 23, 24]. These depend in part on the type of constitutive law that applies to the material under consideration. The simplest approach is the one valid for a material obeying a relation of the type $\sigma(\epsilon, \dot{\epsilon}, T) = f(\epsilon, T) \times g(\dot{\epsilon}, T)$ so that, for a given temperature, the influences of strain and strain rate are expressed separately in a multiplicative way. In such a substance, the normalized strain hardening coefficient $\gamma = (\partial \ln \sigma / \partial \epsilon)_{\dot{\epsilon}}$ is independent of the strain rate $\dot{\epsilon}$ and depends only on the accumulated strain ϵ. Similarly, the strain rate sensitivity coefficient $m = (\partial \ln \sigma / \partial \ln \dot{\epsilon})_{\epsilon}$ is independent of the strain. As demonstrated earlier [7, 8], the plastic behaviour of high density polyethylene can be fitted to a first approximation by the following equation:

$$\sigma(\epsilon, \dot{\epsilon}) = K \exp(h \epsilon^2) \dot{\epsilon}^m. \quad (1)$$

Here the three adjustable coefficients are given by $K = 46$ MPa, $h = 0.41$ and $m = 0.07$. With this constitutive relation, the following $\gamma = \gamma(\epsilon)$ relation is obtained

$$\gamma = 2 h \epsilon. \quad (2)$$

Although the above expression was chosen for simplicity, it is evident from the experimental γ against ϵ curve in Fig. 5 that the description of the dependence of γ on strain can be improved by the addition of an extra term:

$$\gamma = \gamma_0 + 2 h' \epsilon. \quad (3)$$

Allowance must also be made for the short period of viscoelastic flow at the commencement of straining. Although this behaviour is rate dependent, and therefore in conflict with the assumed strain dependence $f(\epsilon, T)$ introduced above, the rate dependence will be neglected here as not being of primary importance with respect to the process of neck propagation under investigation. The full stress/strain relation, including the viscoelastic component, is then given by:

$$\sigma = K V(\epsilon) \exp(h \epsilon^2) \dot{\epsilon}^m \quad (4)$$

where the viscoelastic term $V(\epsilon)$ is defined as:

$$V(\epsilon) = [1 - \exp(-\epsilon/\epsilon_v)] \quad (5)$$

where ϵ_v is about 0.033 in the present case. As long as ϵ_v is considered as independent of the strain rate, the analyses developed for the deformation of metals can be applied to polymer stretching. Then the strain rate gradient $\lambda' = (\partial \ln \dot{\epsilon} / \partial x)_t$ that is present at a particular site x and time t can be specified in terms of the strain rate sensitivity m and the current value of γ by the relation [17]:

$$m\lambda' = (1 - \gamma)\lambda - (\mathrm{d} \ln A_0 / \mathrm{d}x). \quad (6)$$

Here λ is the strain gradient $(\partial \epsilon / \partial x)_t$, and $\mathrm{d} \ln A_0 / \mathrm{d}x$ is the gradient in the natural logarithm of the cross-sectional area prior to the initiation of straining. By convention, the area gradient term $\mathrm{d} \ln A_0 / \mathrm{d}x$ is generally taken to be negative so that the initial values of λ' in different parts of the sample (i.e. when $\lambda = 0$) are normally positive. These lead in turn to the development of positive values of λ at large strains, as depicted in Fig. 6 for three samples of the material of Fig. 5 containing defect gradients

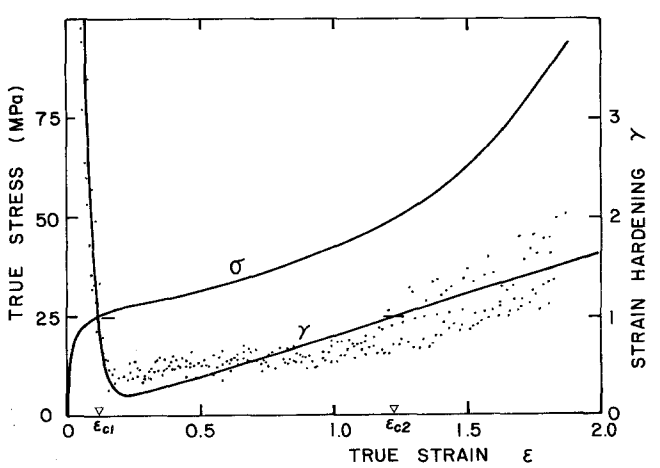

Figure 5 Flow curve of HDPE determined at 21° C and a constant strain rate of 10^{-3} sec^{-1} and plotted in terms of $\ln \sigma$ against true strain ϵ. The dependence of $\gamma = \partial \ln \sigma / \partial \epsilon|_{\dot{\epsilon}}$, i.e. of the slope of the $\ln \sigma$ against ϵ curve, on strain ϵ is also illustrated.

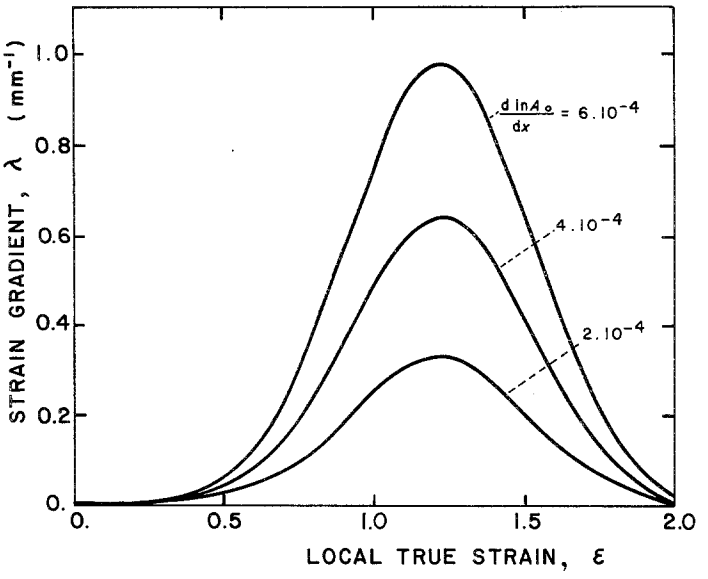

Figure 6 Dependence of $\lambda = |\partial\epsilon/\partial x|_t$ on the local strain ϵ determined by integrating Equation 6 on the basis of the γ against ϵ data of Fig. 5 and Equation 4. The maximum value of λ can be seen to depend on the magnitude of the initial geometric defect.

from 2.0×10^{-4} to 6.0×10^{-4} mm^{-1}. The increase in λ' corresponds to the initiation and development of a well formed neck, as can be verified by comparing Figs. 6 and 7. (In Fig. 7, the data of Fig. 4 have been replotted in terms of $\lambda \simeq \Delta\epsilon/\Delta x$ against $\bar{\epsilon}$, where $\Delta\epsilon$ represents the strain differences between neighbouring slices and $\bar{\epsilon}$ is the mean strain in the two slices being compared.)

It should be noted that λ' takes the value $(-1/m)(\mathrm{d} \ln A_0/\mathrm{d}x)$ (Fig. 6) at the commencement of straining when $\lambda = 0$, and also whenever the strain hardening coefficient $\gamma = 1$ (i.e. at the first and second Considère strains ϵ_{c1} and ϵ_{c2}, Fig. 5). Thus three stages can readily be distinguished in the growth and decay of the strain gradient λ. In the first, which extends over the first few per cent of overall strain until the maximum load is attained (i.e. until the first Considère strain), λ grows slowly, but at a rate which is generally not perceptible to the naked eye. In the second, which extends from the first to the second Considère strain, λ increases rapidly because λ' assumes fairly high values (i.e. $\lambda' \gg (-1/m)(\mathrm{d} \ln A_0/\mathrm{d}x)$) over much of this interval. This corresponds to the period of neck formation at a given site. In the third, $\gamma > 1$ in the vicinity of the original neck, so that λ' decreases to less than $(-1/m)(\mathrm{d} \ln A_0/\mathrm{d}x)$ and actually becomes negative (see Figs. 6

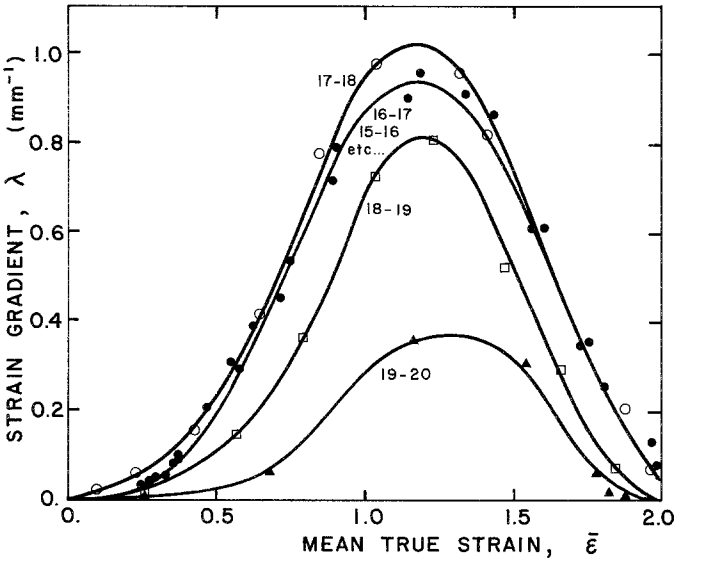

Figure 7 Dependence of $\lambda \simeq \Delta\epsilon/\Delta x$ on the local strain ϵ determined from the experimental data of Fig. 4.

and 7). Under these conditions, λ decreases gradually until it is again hardly perceptible visually. This corresponds to the interval of neck stabilization and propagation. During stretching, this is when the original constriction decreases in diameter only slowly and when the elongation associated with the natural draw ratio is gradually transmitted along the sample axis.

It is clear from Equation 6 that, for given values of γ and $\mathrm{d} \ln A_0/\mathrm{d}x$ (i.e. for a particular shape of σ against ϵ curve and area gradient), the strain rate gradient λ' increases in inverse proportion to the rate sensitivity m. Thus the "draw" is the more localized the lower is the value of m. As a result, once again in contrast to the behaviour of metals (where high m promotes good formability), in polymers, good drawability implies the possession of a low rate sensitivity.

In Fig. 7, there was a clear difference in the behaviour of the strain gradient λ relating to neck slices (i) 19 and 20, 18 and 19; (ii) 17 and 18; and (iii) 16 and 17, 15 and 16, etc. Slices 18, 19 and 20 were located within the original area defect, so they all passed through the "draw" at about the same time; so, the strain gradient $\lambda = \Delta\epsilon/\Delta x$ measured from the pairs of slices 19 and 20, and 18 and 19 increased rather slowly up to moderate values of the order of 0.4 and 0.8, respectively. By contrast, slices 17 and 18, being located the first outside and the second inside the defect, experienced the draw at significantly different intervals of time, and the value of λ was, therefore, considerably higher in the ascending stage of the curve for these two sections. We turn now to slices 16 and 17, 15 and 16, etc., which were all nominally machined to the same diameter D_0. They could, accordingly, be expected to pass through the draw simultaneously. Instead, as is evident from Fig. 7, $\lambda = \Delta\epsilon/\Delta x$ was almost as high in these parts of the sample as in slices 17 and 18 (only a slight difference is noticed near the origin of the graph). It is evident, therefore, that the factor responsible for the propagation of the draw from slice to slice of the uniform part of the sample is missing from Equation 6 and remains to be introduced. As will be demonstrated below, this factor may be related to the transverse compressive stresses generated in the shoulders of the neck. One possible method for the incorporation of such stresses will now be considered, after the addition of a number of further terms to the strain rate gradient relationship.

3.2. Effect on the necking process of the presence of strength and temperature gradients

Although Equation 6 was originally developed to explain the influence of geometric and "deformation" defects [17], it can be readily modified so as to describe the effect of other kinds of sample non-uniformities. For example, when the strength of the material is specified by a simple constitutive relation of the type considered here, which is of the form $\sigma = K\dot{\epsilon}^m f(\epsilon)$, and when the strength coefficient $K = K(x)$ varies along the specimen axis, the term $-\mathrm{d} \ln K/\mathrm{d}x$ can be added to account for the presence of such "strength defects" [18]. Such a term is formally similar to the area gradient term discussed above. It is of particular interest when the area gradient $\mathrm{d} \ln A_0/\mathrm{d}x$ is very small or non-existent. Under such conditions, necking is initiated where the strength of the material is slightly deficient (e.g. 0.5% less) compared to the bulk of the sample. This can arise due to small local differences in the volume fraction of crystallinity, the mean molecular weight, etc.

In a similar manner, it is possible to allow for the presence or development of temperature gradients, as suggested by Ferron [25, 26]. This is done by the addition of the term:

$$-\left(\frac{\mathrm{d} \ln \sigma}{\partial T}\right)_{\epsilon,\dot{\epsilon}} \left(\frac{\partial T}{\partial x}\right)_t \qquad (7)$$

where $(\partial \ln \sigma/\partial T)_{\epsilon,\dot{\epsilon}}$ is the temperature-dependence of the true stress (normally negative), and $(\partial T/\partial x)_t$ is the temperature gradient involved in passing from the "normal" towards the overheated part of the specimen. The temperature gradient term is of particular importance when no other inhomogeneities are present. It is normally associated with the occurrence of adiabatic heating in conjunction with a non-uniform distribution of heat sinks. Once a local temperature gradient is developed in a solid polymer, it is readily propagated to the ends of a specimen, carrying with it the strain localization associated with the draw [27–29].

4. Effect of stress triaxiality on neck propagation

4.1. The effective stress and the Bridgman triaxiality factor

The analysis described in Section 3 above is rigorously valid only when the state of stress is

uniaxial, that is when no radial or circumferential stresses are developed in the stretched bar. This assumption is reasonably valid as long as the tensile deformation is homogeneous and the profile of the specimen remains fairly uniform. Conversely, if the stress tensor deviates from a uniaxial one, so that finite radial and circumferential stresses (σ_r and σ_θ, respectively) are induced in addition to the axial stress σ_x, the plastic behaviour of the specimen must be described instead in terms of the local effective stress σ_{eff} and effective strain ϵ_{eff} [30]. According to this concept, σ_{eff} is numerically equal to that uniaxial stress which would produce the same effective strain rate as the one generated by the complex stress field. The rate of plastic deformation is increased by the triaxiality effect if the transverse stresses are compressive and conversely decreased if the hydrostatic term in tensile. When an axially symmetric specimen containing a defect is deformed in tension beyond the onset of strain localization, the profile becomes highly non-uniform and tranverse components of stress are developed. Since these components usually vary across a given cross-section, it is useful to characterize the overall effect of triaxiality in the section by the mean effective stress $\overline{\sigma_{eff}}$. Following Bridgman [11], we will henceforth denote by the term "triaxiality factor" the ratio $F_T = \overline{\sigma_{eff}}/\bar{\sigma}_x$, where the mean axial stress, $\bar{\sigma}_x = F/A$.

In a tensile specimen with a uniform cross-section the triaxiality factor is equal to 1. If, on the other hand, the specimen profile is curved, F_T is less than or greater than 1 depending on whether the external surface of the sample is concave or convex, respectively (see Fig. 8). Note that, following earlier authors [31–34], the curvature of the individual field of force lines is of the same sign as that of the outer profile. Thus, in the externally concave region, the stresses can only be balanced if σ_r and σ_θ are both positive, so that $F_T < 1$. Conversely, in the externally convex region which is of greater interest to the present discussion, $F_T > 1$.

4.2. Dependence of F_T on the local curvature

To date, no simple analytical expression for F_T has been proposed which is valid for arbitrary

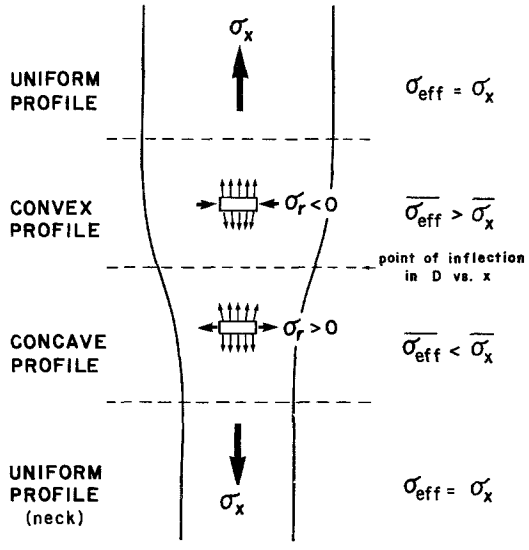

Figure 8 Schematic representation of the transverse stresses generated in a sample of varying cross-section. Note that $\overline{\sigma_{eff}} > \bar{\sigma}_x (F_T > 1)$ in regions of negative curvature.

axi-symmetric profiles. This is because F_T depends in a complex way, not only on the first and second derivatives of the profile radius $a(x')$,* but also on the plastic properties of the material [11]. Nevertheless, several attempts at expressing the effect of triaxiality have been made for the case where the ratio a/R (of the specimen radius a to the radius of curvature of the profile R) is small [11, 33, 35]. Among these, the approach of Bridgman [11] is most relevant to the current study. It was applied to the transverse plane of symmetry at the neck of a tensile bar, where $da/dx' = 0$, and where the radius of curvature R, given by $R = 1/(d^2a/dx'^2)$ when $da/dx' = 0$, is positive. Under these conditions, F_T can be expressed as follows:

$$F_T = 1/[1 + (2R/a)] \ln [1 + (a/2R)] \quad (8)$$

It can be readily shown [9] that the original assumptions of Bridgman remain valid for symmetrically bulged profiles (as well as symmetrically necked profiles) as long as a negative value is attribued to R. By extension, the formula also applies to any section in which the derivative da/dx' is zero, e.g. in the uniform parts of the bar.

The dependence of the Bridgman triaxiality

*The triaxiality effects depend on the current shape of the sample in Eulerian or *laboratory* space. They must therefore be evaluated in these coordinates, which are distinguished here from the former by the use of a primed letter (x') as opposed to a simple x.

factor F_T on the ratio a/R is illustrated in Fig. 9 for both negative as well as positive values of a/R. For very small values of (a/R), that is for a nearly uniaxial state of stress, the logarithmic relation for F_T given by Equation 8 can be developed as a power series in a/R, the first two terms of which lead to

$$F_T = [1 - (a/4R)] \quad (9)$$

It is of interest to note that this expression is the approximate equivalent of the earlier triaxiality correction proposed by Siebel [35] as

$$F_T = 1/[1 + (a/4R)] \quad (10)$$

The Bridgman formulation can also be compared with that of Hutchinson and Obrecht [36], which expresses the influence of the wavelength of a small sinusoidal fluctuation in the external profile on the rate of strain localization in tension. They found that the difference in the rate of decrease in cross-sectional area at the minimum and maximum diameters is less than expected from a simple uniaxial analysis. When converted into the present notation, that is, on reinterpretation in terms of (a/R) ratios and of a triaxiality factor $\overline{\sigma_{eff}}/\overline{\sigma_x}$, their result also tends to the value $[1 - (a/4R)]$ for small (a/R), giving additional support to the concept of extending the Bridgman analysis to negative values of (a/R).

For the present purpose, the validity of Equation 8 is restricted to small values of the (a/R) ratio, namely $|a/R| < 1$, by virtue of an extension of St Venant's principle [37]. That is we adopt the view here that the effect of a "surface irregularity", such as positive or negative curvature, does not extend in a significant way beyond a depth about equal to some geometric characteristic of the irregularity, in this case the radius of curvature.

In the experimental profiles shown in Fig. 2 for the HDPE rod stretched at room temperature, the ratio a/R fell in the range -0.5 to 0.2, and therefore within the limitations imposed by the "surface effects". Furthermore, by means of finite element calculations, it has been shown [38] that Equation 8 is a reasonable approximation of the effect of triaxiality on the effective stress, at least in regions of symmetry. It is not immediately apparent, however, that Equation 8 continues to apply in regions where the profile or area gradient is not zero. In such parts of the sample, the expression for F_T could include, for example, terms in (da/dx'). Support for the view that the Bridgman relation is of at least approximate validity under these conditions can be taken from the work of Argon *et al.* [39], who employed a finite element method to show that the expressions for σ_{rr} and $\sigma_{\theta\theta}$ given by the Bridgman analysis continue to apply along the axis of symmetry. From their work, it can be concluded that Equation 8 is a good first approximation for the actual triaxiality factor, even when $da/dx' \neq 0$. Somewhat similar conclusions were drawn by Ghosh [31] for the case of metal sheets which experience tensile necking.

4.3. Influence of the triaxiality factor on kinetics of plastic strain localization

In the derivation of the differential equation (Equation 6) relating the strain and strain rate gradients to the material coefficients and non-uniformities, the relevant stress was the uniaxial tensile stress, as is normally the case for the so-called "long wavelength" approximations [36].

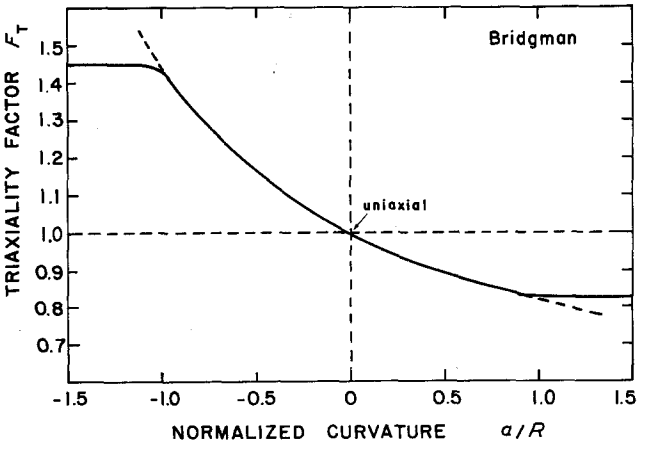

Figure 9 Dependence of Bridgman triaxiality correction factor F_T on (a/R). The extension of Bridgman's relation for F_T into the region of negative (a/R) is limited to $(a/R) \geqslant -1$ because of St. Venant's principle [37].

However, in the present instance, the tensile force per unit of current cross-section must be expressed in terms of the longitudinal component σ_x of the axially oriented principal stress. In what follows, we will not be concerned with the radial variation in this quantity, but consider only its average value, $\bar{\sigma}_x$. Recalling that $\bar{\sigma}_x = \overline{\sigma_{eff}}/F_T$, we can represent the effect of differences in F_T along the axis of an otherwise uniform sample, for example, by the expression:

$$\delta \ln \bar{\sigma}_x = \delta \ln \overline{\sigma_{eff}} - \delta \ln F_T \qquad (11)$$

In order to extend the instability analysis to include the effect of triaxial stresses, the following assumptions will now prove useful:

(i) The increment in the mean effective strain $d\overline{\bar{\epsilon}_{eff}}$ is taken as approximately equal to the increment in the mean longitudinal strain $d\bar{\epsilon}_x$.

(ii) Although the strain hardening (and rate sensitivity) properties of the material depend on the mean effective strain (and mean effective strain rate), these can be deduced to a sufficient degree of accuracy from the mean longitudinal strains (and strain rates).

Under these conditions, Equation 6 can be relaced by:

$$m\lambda' = (1-\gamma)\lambda - \frac{d \ln A_0}{dx} + \left(\frac{\partial \ln F_T}{\partial x}\right)_t \qquad (12)$$

From the above relation, it can be seen that the triaxiality term $(\partial \ln F_t/\partial x)_t$ is formally equivalent to the other types of non-uniformities considered in turn above*. The magnitude and therefore the importance of this term can be estimated from Fig. 9. For this purpose we consider two neighbouring regions of equal cross-section, one of which is of uniform radius ($da/dx' = 0$; $a/R = 0$; $F_T = 1.0$), and the other of which has a small negative curvature (e.g. $a/R = -0.12$; $F_T = 1.04$). It is evident that $\delta \ln F_T$ in this instance is equivalent to an area defect $\delta \ln A_0$ of 4%. The validity of this simple estimate is supported by the photographs of Fig. 2, and by the local strain curves of Fig. 4, from which it can be seen that the delay in the propagation of the constriction from "slice" to "slice" of the uniform part of the specimen is equivalent to the presence of an area defect of something less than 5%.

Thus the triaxiality term in Equation 12 provides a ready explanation for the observation that a neck, once formed, generally propagates in an orderly fashion towards the ends of a polymer specimen, instead of being reinitiated at small "strength" defects along the so-called "uniform" portion of the unconstricted parts of the specimen. This is because the negative curvature at the ends of such regions has a large enough effect, according to the instability analysis, to provoke deformation at this location, rather than in the less inhomogeneous regions of the sample.

5. Conclusions

1. The times associated with neck initiation and stabilization in high density polyethylene correspond to moments when the normalized strain hardening coefficient γ passes through the critical value $\gamma = 1$.

2. The progress of strain localization in solid polymers can be quantified in terms of the local values of the strain and strain rate gradients. According to this treatment, the rapidity of neck development is inversely proportional to the rate sensitivity m of the material. Also playing a role in the necking behaviour are the various types of defect present, which include non-uniformities in cross-sectional area, intrinsic strength, local temperature, and prestrain history. These inhomogeneities are responsible for the site of the first localization, and also contribute to the rate of its stabilization.

3. The propagation of a constriction along an otherwise uniform section of the sample can be explained in terms of the transverse compressive stresses developed at the current shoulders of the neck. The effect of these triaxial stresses can be quantified in terms of a modified Bridgman correction factor, which is seen to be valid in locations of negative as well as positive curvature. In the presence of variations in cross-section, the gradient in the Bridgman triaxiality factor must be added to the strain localization relationship and plays a role analogous to that of an area or strength defect.

Acknowledgements

The authors are indebted to the following organizations for the provision of travelling fellowships:

*Note, however, that the area and strength defects $d \ln A_0/dx$ and $d \ln K/dx$ are initial conditions which are independent of the time t, whereas the temperature (Equation 7) and triaxiality gradients evolve with time, and eventually disappear.

the Ministry of Education of France (NAH); the Ministry of External Relations of France (CG's); the Ministry of Intergovernmental Affairs of Quebec (JJJ).

References

1. S. W. ALLISON and I. M. WARD, *Brit. J. Appl. Phys.* 18 (1967) 1151.
2. J. M. ANDREWS and I. M. WARD, *J. Mater. Sci.* 5 (1970) 411.
3. A. J. DE VRIES, *Pure Appl. Chem.* 53 (1981) 1011.
4. E. W. HART, *Acta Metall.* 15 (1967) 351.
5. A. S. ARGON, in "The Inhomogeneity of Plastic Deformation" (ASM, Metals Park, 1973) p. 161.
6. U. F. KOCKS, J. J. JONAS and H. MECKING, *Acta Metall.* 27 (1979) 419.
7. C. G'SELL and J. J. JONAS, *J. Mater. Sci.* 14 (1979) 583.
8. *Idem, ibid.* 16 (1981) 1956.
9. N. A. ALY-HELAL, Thèse de Docteur-Ingénieur, INPL, Nancy (1982).
10. C. G'SELL and N. A. ALY-HELAL, to be published.
11. P. W. BRIDGMAN, *Trans. Amer. Soc. Met.* 32 (1944) 2024.
12. S. J. NEWMANN, *J. Appl. Phys.* 2 (1959) 252.
13. P. I. VINCENT, *Polymer* 1 (1960) 7.
14. G. MEINEL, N. MOROSOFF and A. PETERLIN, *J. Polym. Sci. A2* 8 (1970) 1723.
15. G. MEINEL and A. PETERLIN, *ibid.* 9 (1971) 145.
16. M. WADA and T. NAKAMURA, *Phil. Mag.* A38 (1978) 167.
17. J. J. JONAS, R. A. HOLT and C. E. COLEMAN, *Acta Metall.* 24 (1976) 911.
18. J. J. JONAS, N. CHRISTODOULOU and C. G'SELL, *Scripta Metall.* 12 (1978) 565.
19. I. H. HALL, *J. Appl. Polym. Sci.* 12 (1968) 731.
20. M. WADA, T. NAKAMURA and N. KINOSHITA, *Phil. Mag.* A38 (1978) 167.
21. A. PETERLIN, *J. Mater. Sci.* 6 (1971) 490.
22. S. S. HECKER, A. K. GHOSH and H. L. GEGEL, "Formability, Analysis, Modeling and Experimentation" (AIME, USA, 1982).
23. J. J. JONAS and B. BAUDELET, *Acta Metall.* 25 (1977) 43.
24. N. CHRISTODOULOU and J. J. JONAS, *Res. Mechanica* 5 (1982) 49.
25. G. FERRON, *Mater. Sci. Eng.* 49 (1981) 241.
26. *Idem, ibid.* 52 (1982) 133.
27. I. MARSHALL and A. B. THOMPSON, *J. Appl. Chem.* 4 (1954) 145.
28. G. I. BARENBLATT, *Rheol. Acta* 13 (1974) 924.
29. K. JÄCKEL, *Kolloid Z.* 137 (1954) 130.
30. G. E. DIETER, "Mechanical Metallurgy" (McGraw Hill, New York, 1961) p. 90.
31. A. K. GHOSH, *Metall. Trans. A* 8 (1977) 1221.
32. D. M. NORRIS Jr., B. MORAN, J. K. SCUDDER and D. F. QUINONES, *J. Mech. Phys. Solids* 26 (1978) 1.
33. N. N. DAVIDENKOV and N. I. SPIRIDONOVA, *Proc. Amer. Soc. Test. Mater.* 46 (1946) 1147.
34. N. KASAI and M. KAKUDO, *J. Polym. Sci.* A2 (1964) 1955.
35. E. SIEBEL, *Werkstoffausschuss* 71 (1925) 5.
36. J. W. HUTCHINSON and H. OBRECHT, in "Fracture, 1977", Proceedings of the International Conference on Fracture 4, Waterloo, Canada, Vol. 1, edited by D. M. R. Taplin (1977) 101.
37. B. DE SAINT-VENANT, Mem. des Savants Etrangers, Tome 14 (Paris, 1856) pp. 233–560.
38. A. NEEDLEMAN, *J. Mech. Phys. Solids* 20 (1972) 111.
39. A. S. ARGON, J. IM and A. NEEDLEMAN, *Metall. Trans.* 6A (1975) 815.

Received 1 October
and accepted 12 November 1982